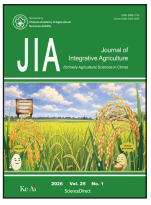
Journal of Integrative Agriculture 2026, 25(1): 192–206

Available online at ScienceDirect

Journal of Integrative Agriculture



RESEARCH ARTICLE

MicroRNA-mediated modulation of immune genes facilitates *Metarhizium anisopliae* infection in the red imported fire ant, *Solenopsis invicta*

Yating Xu[*], Junaid Zafar[*], Liangjie Lin, Hongxin Wu, Zehong Kang, Jie Zhang, Rana Fartab Shoukat, Yongyue Lu, Rui Pang, Fengliang Jin[#], Xiaoxia Xu[#]

State Key Laboratory of Green Pesticide "Belt and Road" Technology Industry/Innovation Institute for Green and Biological Control of Agricultural Pests/ College of Plant Protection, South China Agricultural University, Guangzhou 510642, China

Highlights

- Spatiotemporal profiling of host-encoded microRNAs revealed dynamic regulation of immune pathways in *Metarhizium anisopliae*-infected *Solenopsis invicta*.
- MiR-71 and miR-7 regulated key immune pathway genes through direct targeting of *ModSP1-Relish* and *Lysozyme2-Serine protease7*, respectively.
- Manipulation of miR-71 and miR-7 impaired antifungal immunity and enhanced susceptibility to infection, offering insights for improved mycoinsecticide development.

Abstract

The red imported fire ant, *Solenopsis invicta* Buren, is a highly invasive eusocial insect pest that threatens native biodiversity, agriculture, and human health. The innate immune system and intricate social immune responses of *S. invicta* pose challenges to the development of effective control strategies. MicroRNAs (miRNAs) play critical roles in the post-transcriptional regulation of gene expression, which influences various biological processes, including immunity and host-pathogen interactions. While the miRNA-mediated response of insects to pathogens has been extensively studied in solitary insects, little is known about the innate immune responses of individual members within a colony. To address this gap, we constructed small RNA libraries from *Metarhizium anisopliae*-infected *S. invicta* workers and investigated the temporal dynamics of miRNA-mediated immune responses to the entomopathogen. Several differentially expressed miRNAs were identified, and they were found to regulate genes involved in the Toll, IMD, and melanization immune pathways. Quantitative real-time PCR (qRT-PCR) was employed to analyze the spatiotemporal dynamics of key miRNAs/target genes, specifically miR-71/*ModSP1-Relish* and miR-7/*Lysozyme2-Serine protease7*. A dual luciferase assay (*in vitro*) was performed to validate the interactions between miRNAs and their target genes. Overexpression of miR-71 and miR-7 (*via* miRNA mimics) efficiently suppressed their target genes, impaired the antifungal immune response of *S. invicta* and increased the susceptibility to *M. anisopliae* infection compared to controls. Furthermore, RNA interference-based gene silencing elucidated the roles of these immune genes in regulating fungal susceptibility, thus providing vital clues for developing virulent and effective mycoinsecticides using modern genetic engineering tools.

Keywords: fire ants, microRNAs, RNAi, host-pathogen, innate immunity, entomopathogenic fungi

1. Introduction

The red imported fire ant, *Solenopsis invicta* (Buren) (Hymenoptera: Formicidae), is an economically important eusocial invasive pest that has substantial impacts on global ecosystems, agriculture, and human health (Menchetti *et al.* 2023). Chemical insecticides are currently the primary option for managing *S. invicta* infestations (Sakamoto and Goka 2021; Liang *et al.* 2023), but their widespread use imbalances the ecosystem and contaminates soil, while spawning insecticide-resistant strains (Zhang *et al.* 2023).

Received 28 October 2024; Received in revised form 1 December 2024; Accepted 20 December 2024; Available online 10 February 2025
Yating Xu, E-mail: xuyt1101@stu.scau.edu.cn; Junaid Zafar, E-mail: jz_jaam@yahoo.com; [#]Correspondence Fengliang Jin, E-mail: jflbang@scau.edu.cn; Xiaoxia Xu, E-mail: xuxiaoxia111@scau.edu.cn
[*] These authors contributed equally to this study.

© 2026 CAAS. Publishing services by Elsevier B.V. on behalf of KeAi Communications Co. Ltd. This is an open access article under the CC BY-NC-ND license (http://creativecommons.org/licenses/by-nc-nd/4.0/). Peer review under responsibility of Editorial Board of *Journal of Integrative Agriculture*.
doi: 10.1016/j.jia.2025.02.009

These concerns have driven the search for effective, safe, and sustainable biological control agents.

Eusocial insects live in an intricately structured social system with a division of labor, including worker castes that are responsible for foraging and defending the colony (Cremer *et al.* 2007). Despite the benefits of eusociality, communal living fosters an environment conducive for the growth and spread of microorganisms, which may jeopardize the survival of the entire colony. The ambient temperature, hospitable humidity, susceptible immatures, and frequent contact between nestmates provide ideal conditions for the proliferation of pathogens (Feldhaar and Gross 2008). *Beauveria bassiana* and *Metarhizium anisopliae* are two widely used entomopathogenic fungi that can potentially exploit these favorable colony conditions, making them effective microbial insecticides for managing *S. invicta* (Tschinkel 2013). Once foragers outside the colony become contaminated, they can spread the infectious spores to their nestmates, leading to the demise of the colony (Cremer *et al.* 2007). Fungal pathogenesis is moderately slow for controlling insects compared to chemical insecticides partly due to host immune defenses (Scholte *et al.* 2005; Fang *et al.* 2012), which has restricted their widespread application. Understanding the fungus-induced immune responses could provide vital clues for developing virulent, ecofriendly and efficient mycoinsecticides *via* modern genetic engineering tools (Wang and Wang 2017).

Ants have evolved numerous defensive strategies, from broad-scale social immunity comprising trophallaxis (Qiu *et al.* 2016), necrophoresis (Qiu *et al.* 2015), and grooming behaviors (Qiu *et al.* 2014) to individual innate immune responses (Schmid-Hempel 2005). The innate immune system recognizes pathogen-associated molecular patterns (PAMPs) by binding host-derived pattern recognition receptors (PRRs) (Hillyer 2016), subsequently initiating signaling pathways which require the activation of transcription factors and changes in gene expression (Lu and Leger 2016). The Toll and IMD pathways are central to immune responses against microbial infections (Yang *et al.* 2023). The Toll pathway primarily targets fungal pathogens and Gram-positive bacteria by activating NF-κB transcription factors such as Dorsal and Dif to regulate immunity (Zheng *et al.* 2020). Meanwhile, the IMD pathway is mainly responsive to Gram-negative bacteria, but it also plays a role in antifungal defense through the activation of Relish, another NF-κB transcription factor (Geng *et al.* 2021). Knockdown of *PpTollA* and *PpIMD* in *Pteromalus puparum* significantly enhanced fungal proliferation, reduced survival rates, and suppressed antimicrobial peptide expression (Yang *et al.* 2023). Such host-pathogen interactions lead to broad immunological dysfunctions in host cells. Strict regulation of immune pathways is crucial for reducing fitness costs and maintaining immune homeostasis (Lucas *et al.* 2015).

MicroRNAs (miRNAs) are small non-coding RNAs (~22 nucleotides) that play crucial roles in the post-transcriptional regulation of gene expression, thereby impacting several biological processes, including immunity and host-pathogen cross-talk (Asgari 2018). Pathogenic infections can alter the expression profile of host miRNAs, potentially shaping the host immune response or facilitating pathogen replication. For instance, *Micrococcus luteus* infection in *Drosophila* induces the differential expression of several miRNAs enriched in various immune signaling pathways such as Toll and IMD (Wei *et al.* 2018). In *Tribolium castaneum*, microbial stress caused changes in miRNA expression (Freitak *et al.* 2012). Conserved miR-8 suppression in the diamondback moth upregulates *Serpin* 27, a negative regulator of the Toll and PPO pathways (Etebari and Asgari 2013). These alterations can be pathogen species-specific, with some miRNAs being suppressed by one pathogen and overexpressed by another closely related species (Asgari 2011). For example, in *Galleria mellonella*, larval diets contaminated with the pathogenic bacterium *Serratia entomophila* resulted in the downregulation of api-miR-263a, whereas non-pathogenic *Escherichia coli* induced upregulation (Mukherjee and Vilcinskas 2014). Some studies have shown differences between the immune responses of solitary and social insects. Early genomic studies found that honey bees have fewer immunity genes than fruit flies and mosquitoes (Evans *et al.* 2006). While the miRNA-mediated insect response to pathogens is well-studied in solitary insects on an immunological level (Lu and Leger 2016), a gap remains in our understanding of the innate immune responses of the individual members in a colony.

In the current study, we investigated the immuno-modulatory role of miRNAs in eusocial insects using a "host–pathogen" system. We employed RNA-seq to profile *M. anisopliae*-induced miRNAs in *S. invicta* at different intervals. Using bioinformatic tools, we identified several miRNAs that target immune genes, particularly in the Toll and IMD pathways, and constructed interaction networks for these miRNAs. Furthermore, we used various *in vitro* and *in vivo* molecular approaches to functionally verify these interactions.

2. Materials and methods

2.1. Insects, pathogenic fungus, and cell culture

Solenopsis invicta were collected from Huangpu District in Guangzhou, Guangdong Province, China, and maintained in a 20 L plastic container (internally coated with Fluon® (AGC Chemicals, Tokyo, Japan) to prevent escape) at 26°C, 70% relative humidity (RH) and a 12 h light:12 h dark photoperiod, as described in our previous studies (Zafar *et al.* 2023). Worker ants comprise the largest proportion of the colony population. Major workers (head width>1.0 mm) are the largest ants in the colony, with strong jaws and responsibility for defense (Chen *et al.* 2022), and were used for all experiments. The fungal entomopathogen *M. anisopliae* (strain MaqS1902), kindly provided by Prof. Qiongbo Hu (South China Agricultural University, China), was cultivated on potato dextrose agar (PDA) for two weeks and kept in total darkness at (26±1)°C and 75–80% RH. The conidia were harvested into 0.05% Tween-80 (Sigma Aldrich, Darmstadt, Germany) solution and the desired concentrations were prepared (Wu *et al.* 2023).

HEK293T cells were cultured in Dulbecco's Modified Eagle Medium (DMEM; Gibco, Grand Island, NY, USA)

supplemented with 10% fetal bovine serum (FBS), and incubated at 37°C in a 5% CO_2 atmosphere.

2.2. Fungal infection and small RNA library construction

For the fungal infection, *S. invicta* (major workers, 30/replicate×3 replicates/assay), were exposed to *M. anisopliae* suspensions (1×10^8, 1×10^7, 1×10^6, 1×10^5, and 1×10^4 conidia mL^{-1}) *via* immersion and placed onto filter paper to absorb the surplus liquid on the body surface, as described in our previous studies (Wu *et al.* 2023). Ants in the control groups were treated with 0.05% Tween-80 (Zhang *et al.* 2021). The survival rates were monitored daily, and dead ants were placed in a humid chamber to confirm fungal infection.

For small RNA-seq, ants were infected with 5×10^7 conidia mL^{-1} (LC_{50}). Whole-body samples from the control (0 h) and *M. anisopliae*-infected (6, 24, and 48 h) groups were collected. The total RNA was extracted from the control and *M. anisopliae*-infected samples using a TRIzol™ Reagent Kit (Invitrogen, CA, USA). For each sample, 1 μg of total RNA was used as the input into the Illumina TruSeq Small RNA Sample Preparation Kit (Illumina, CA, USA). Briefly, RNA molecules in the size range of 18–30 nt were enriched by polyacrylamide gel electrophoresis (PAGE). The 3′ adapters were added, enriching the 36–48 nt RNAs. The 5′ adapters were then ligated to the RNAs. The resulting ligation products were reverse transcribed *via* PCR amplification, and the PCR products in a size range of 140–160 bp were enriched to create cDNA libraries. The constructed libraries were tested for quality and yield using an Agilent 2100 Bioanalyzer and an ABI StepOnePlus™ Real-Time PCR System (Life Technologies, Inc., Carlsbad, CA, USA). Finally, the libraries were sequenced using Illumina HiSeq X Ten by Gene Denovo Biotechnology Co. (Guangzhou, China).

2.3. Bioinformatic analysis of small RNAs

To obtain the clean reads, the following filtering process was employed: (1) Eliminate low-quality reads (Q-value≤20) and reads containing >10% unknown nucleotides (N); (2) remove reads without 3′ adapters; (3) filter out reads shorter than 18 nt or longer than 30 nt. Then, identical reads were combined from the raw sequences to reduce redundancy. Subsequently, trimmed sequences were aligned to the GenBank (release 209.0) and Rfam (release 11.0) databases to identify and remove the sequences of ribosomal RNA (rRNA), small cytoplasmic RNA (scRNA), small nucleolar RNA (snoRNA), small nuclear RNA (snRNA) and transfer RNA (tRNA). High-quality clean reads were mapped to the *S. invicta* genome (https://www.ncbi.nlm.nih.gov/data-hub/genome/GCF_016802725.1/) using Bowtie (version 1.1.2). Next, we aligned the clean reads with the mature sequences in the miRbase database (version 22) (http://www.mirbase.org/) to identify known miRNAs, while novel miRNAs were identified using the miRDeep2 package (Friedländer *et al.* 2011).

The total miRNA expression level was then calculated and normalized to transcripts per million (TPM). The edgeR software package (Robinson *et al.* 2009) was used to estimate the differences between the control and *M. anisopliae*-infected groups. The miRNAs with TPM≥10; $|\log_2FC|\geq0.58$, and $P<0.05$ were determined to be significantly differentially expressed between the control and infected groups.

2.4. Target gene prediction, functional enrichment, and construction of the miRNA/target gene interaction networks

Our recently published datasets were analyzed to identify the potential targets of differentially expressed miRNAs, where the same *M. anisopliae*-infected *S. invicta* samples were sequenced for mRNAs (Wu *et al.* 2023). The TargetScan (Lewis *et al.* 2005) and miRanda (Betel *et al.* 2010) algorithms were employed to predict the potential target genes of differentially expressed miRNAs. The negatively co-expressed miRNA–mRNA pairs with Pearson correlation coefficient (PCC)≤–0.4 and $P<0.05$ were retained. The predicted miRNA targets were annotated using the Kyoto Encyclopedia of Genes and Genomes (KEGG) and Gene Ontology (GO) databases. Genes annotated as hypothetical or unknown proteins were excluded. Cytoscape (3.10.1) (https://cytoscape.org/) software was used to generate, visualize and analyze the immune-related miRNA-mRNA interaction networks.

2.5. Quantitative real-time PCR (qRT-PCR)

Total RNA was extracted from different tissues (head, thorax and abdomen) and life stages/castes (eggs, larvae, pupae, major, medium, minor, male, and female), using TRIzol (Omega, USA). The first-strand cDNA was synthesized using the Color Reverse Transcription Kit (EZBioscience, Beijing, China), and the miRNA reverse transcription reaction was performed with the MiR-XTM miRNA First-strand Synthesis Kit (TaKaRa, Tokyo, Japan) following the manufacturer's guidelines. qRT-PCR was performed using 200 ng of cDNA and TB Green Premix *ExTaq* (TaKaRa, Tokyo, Japan) with three technical replicates on a CFX96™ real-time PCR detection system (Bio-Rad, Hercules, CA, USA). The ribosomal protein 13 (*RPL13*) and *U6* served as internal reference controls. The primers used in this study are listed in Appendix A.

2.6. Dual-luciferase reporter (DLR) assay

The miRNA-binding regions in the target genes (*Lysozyme2*, *Hymenoptaecin2*, *ModSP1*, *Relish*, *IMD*, *Serine protease7*, *GNBP1*, *GNBP3*, *Toll3* and *PPO1*) were amplified and cloned into a psiCHECK-2 vector (Promega, Madison, WI, USA) containing the *Xho*I and *Pme*I restriction enzyme sites. HEK293T cells were co-transfected with 800 ng of the luciferase reporter vector psiCHECK-2-target and the miRNA mimics or negative control (NC) at a 1:3 ratio using FuGENE® HD transfection reagent (Promega, Madison, WI, USA). The firefly and Renilla luciferase activities were measured after 48 h of transfection with the Dual-Glo Luciferase® Assay System (Promega, Madison, WI, USA) using a luminometer. The results are presented as the ratio of Renilla/firefly luciferase activity. The sequences of the miRNA mimics and

NC are listed in Appendix A.

2.7. Overexpression/inhibition of miRNAs

Solenopsis invicta major workers (50/replicate×3 replicates/assay) were collected from a single colony and placed in a cylindrical container (80 mm×100 mm) with Fluon®-coated inner walls (AGC Chemicals, Tokyo, Japan). The container had a 4 cm layer of wet sand to maintain moisture, followed by a 2 cm layer of plaster. Ants were starved for 24 h and subsequently provided with 20% honey water solution containing either miRNA mimic, inhibitor, or NC (0.2 μg μL^{-1}) (Chen *et al.* 2022), and then challenged with *M. anisopliae* 48 h later. Diets were refreshed daily. The sequences of the miRNA mimic/inhibitor and NC are listed in Appendix A.

2.8. RNA interference

For RNAi-mediated silencing of *Relish*, *ModSP1*, *Serine protease7* and *Lysozyme2*, the DNA templates used for double-stranded RNA (dsRNA) synthesis were amplified by PCR using gene-specific primers with the T7 RNA polymerase-binding site (5′-GGATCCTAATACGACTCACTATAGG-3′) attached to the 5′-end of each primer (Appendix A). The dsRNA was synthesized using a T7 RiboMAX Express RNAi Kit (Promega, Madison, WI, USA) according to the manufacturer's instructions. Green fluorescent protein (GFP) dsRNA (ds*GFP*) was used as a control (GenBank: AF324407.1).

2.9. Data analysis

All the results were obtained from at least three independent experiments. Data were analyzed using one-way analysis of variance (ANOVA) with SPSS 25 (IBM Corp., Armonk, NY, USA), and graphs were designed using GraphPad Prism 10 software (GraphPad, San Diego, CA, USA). Data with $P<0.05$ were generally accepted as statistically significant.

3. Results

3.1. Survival assays and overview of small RNA sequencing

Our findings showed that higher fungal concentrations (1×10^8, 1×10^7 and 1×10^6 conidia mL^{-1}) resulted in the lowest survival rates (16.43, 43.33 and 65.10%) compared to the control group (98.62%) (Fig. 1-A). The dead carcasses showed that *M. anisopliae* had successfully colonized the *S. invicta*, confirming the fungal pathogenicity (Fig. 1-B–G).

Small RNA libraries were constructed for the 0, 6, 24, and 48 h samples. The length distribution of small RNAs in all libraries showed that most RNAs were between 18 and 30 nt, with 20–24 nt being the most abundant (Appendix B). Statistics for the small RNA libraries, including the numbers of raw and clean reads and the distribution of reads among various RNA classes (e.g., tRNA, rRNA, mRNA and miRNA), are provided in Appendix C. Bioinformatic analysis was performed to identify the *M. anisopliae*-induced miRNAs in *S. invicta* at all time intervals and compare them to control. By blasting against miRbase, we identified 54, 56, and 50 known miRNAs in our libraries. The novel miRNAs numbered 18, 30, and 18 at each time point, respectively, compared to the control (Appendix D-a).

3.2. Identification of differentially expressed miRNAs

In total, 65 miRNAs (49 known and 16 novel) showed differential expression patterns (TPM≥10; $|\log_2FC|\geq0.58$, and $P<0.05$) in at least one group. Our results indicated that 23

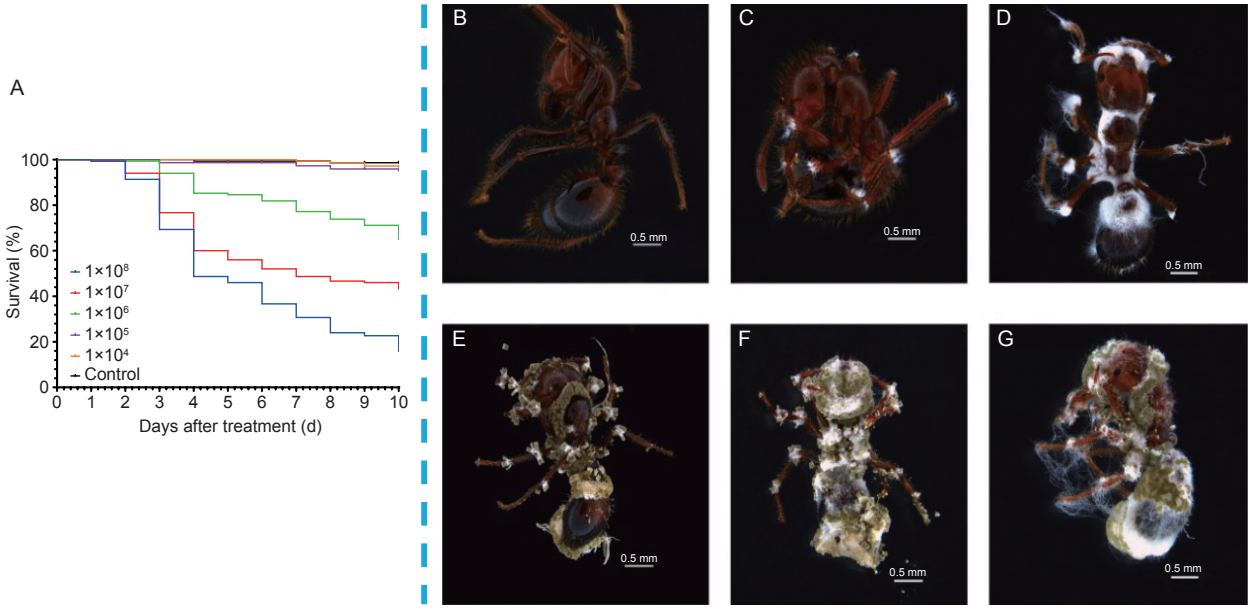


Fig. 1 Pathogenicity of *Metarhizium anisopliae* in *Solenopsis invicta*. A, survival percentage of *S. invicta* (*n*=30/replicate×3 replicates/assay) in response to different concentrations of *M. anisopliae* and the control (0.05% Tween-80). B, an infected ant with no visible fungal growth. C, early signs of external fungal growth, appearing as white spots. D, rapid fungal spread, covering portions of the ant's body. E, severe colonization with extensive fungal growth. F, near-complete coverage of the body by fungus. G, an ant almost entirely covered, with visible green muscardine on the cadaver. Scale bar=0.5 mm.

(19 upregulated and four downregulated), 48 (25 upregulated and 23 downregulated), and 28 (17 upregulated and seven downregulated) miRNAs were differentially expressed at 6, 24, and 48 h, respectively, compared to the control (Appendix D-b). Hierarchical clustering analysis revealed the sample specificity of differentially expressed miRNAs between the control and *M. anisopliae*-infected groups. The miRNAs, including miR-29-5p, miR-10018-5p, miR-184-3p, miR-11-5p, miR-71, and miR-14-5p, exhibited high expression levels at 6 h compared to the control. At 24 h post-infection, miR-133, miR-14-3p, miR-9-3p, miR-99-5p and miR-932-5p were highly expressed, while some miRNAs such as novel-m0036-5p, novel-m0012-3p, miR-13-5p, miR-486-5p, miR-965-3p, miR-7, miR-190-5p and miR-6497-5p displayed abundant expression at 48 h post-infection. A few miRNAs, including miR-71-5p, miR-34-5p and novel-m0049-5p, were upregulated at both 6 and 24 h-post infection compared to the control (Appendix D-c). Notably, 19 differentially expressed miRNAs were shared between the different comparison groups (Appendix D-d).

We randomly selected 13 miRNAs, i.e., miR-263-3p, miR-2-5p, miR-6001-5p, miR-279-5p, novel-m0043-5p, miR-9993-3p, novel-m0012-3p, miR-7975, miR-71-5p, novel-m0049-5p, miR-71, miR-7, and miR-1175-3p, and validated the RNA-seq findings using qRT-PCR (Appendix E-a–c). The results showed similar expression trends and consistency with the RNA-seq analysis, but with some slight discrepancies, such as an opposing trend in the expression of novel-m0012-3p at 6 h, most likely due to the differences between the two techniques.

3.3. Target gene prediction of the differentially expressed miRNAs and functional enrichment analysis

The miRNA-mRNA regulatory interaction analysis revealed 11,599 potential target pairings between the 65 differentially expressed miRNAs and 1,313 differentially expressed genes (Appendix F). Given that miRNAs predominantly act as negative regulators of gene expression, we focused on calculating the negatively correlated miRNA-mRNA interactions which resulted in 1,633 pairings. The rationale for limiting this analysis was to focus solely on interactions that potentially suppress the immune response in *S. invicta* during *M. anisopliae* infection since miRNAs target mRNA cleavage or translational repression (Bartel 2004).

To functionally characterize the target genes of these miRNAs, we performed GO annotation and KEGG pathway enrichment analysis (Appendix G). The GO analysis annotated the genes into three broad categories: biological process, cellular component, and molecular function, with numerous genes enriched in specific sub-categories, i.e., cellular processes, response to stimulus, signaling, immune system process (biological process), cell, macromolecular complex, catalytic activity (cellular component), and catalytic activity, binding, antioxidant activity (molecular function) (Appendix G-a). Based on the KEGG pathway analysis, the Toll and the IMD signaling immune pathways appeared to be the primary responders to *M. anisopliae* infection in *S. invicta* (Appendix G-b). The miRNA-mRNA immune-related interaction networks were generated and analyzed (Fig. 2). Several miRNAs were found to regulate immune genes from the Toll, IMD and melanization pathways. These included genes related to recognition (*GNBP1*, *GNBP3*, *SCARB1*, *PGRP-SA1*, and *PGRP-SA2*), intracellular signaling (*IMD*, *Relish*, *Toll3*, *Cactus*, *Ankyrin*, *ModSP1*, and *ModSP2*), melanization (*Serine protease1*, *Serine protease2*, *Serine protease3*, *Serine protease4*, *Serine protease5*, *Serine protease7*, *PPO1*, *Serpin1*, *Serpin2*, *Serpin3*, *Serpin4*, and *PPAF*) and antimicrobial peptides (*lysozyme2*, *lysozyme3*, *Hymenoptaecin1* and *Hymenoptaecin2*) (Fig. 2-A). Maximum expression levels of most of these immune genes were observed at 48 h post-infection, as evidenced by the gene expression heat map (Fig. 2-B), likely indicating an increased fungal load and an orchestrated response of the immune system to combat infection. A schematic representation of *M. anisopliae*-responsive *S. invicta* immune genes from the Toll, IMD, and melanization pathways is provided in Fig. 2-C. All of the immune-related miRNAs-target gene interactions, including sequences, target sites, gene ID, and functional descriptions, are listed in Appendix H.

3.4. *In vitro* DLR validation of the miRNA-target immune gene interaction

We conducted an *in vitro* DLR assay to assess whether the miRNAs could regulate the expression of their putative target immune genes by acting on their predicted binding sites. Multiple highly expressed immune-related miRNAs, i.e., miR-71-5p (targeting *ModSP1*, *Relish*, *Lysozyme2*, and *Hymenoptaecin2*) miR-29-5p (targeting *IMD* and *GNBP3*), miR-7 (targeting *Serine protease7* and *Lysozyme2*), miR-9-3p (targeting *GNBP1*), miR-971-3p (targeting *PPO1*) and novel-m0019-3p (targeting *Toll3*), were selected (Fig. 3). The predicted binding sites of the miRNAs in their target immune genes are presented in Appendix I.

The DLR assay demonstrated that most of the miRNAs negatively regulated the expression of their predicted target genes. Specifically, miR-71-5p significantly suppressed the expression of *ModSP1* and *Relish*, which are both associated with signal transduction (Fig. 3-A). In addition, miR-7 significantly downregulated *Serine protease7*, a crucial proteolytic enzyme, and *Lysozyme2*, an antimicrobial peptide (Fig. 3-C). Gram-negative binding protein 3 (*GNBP3*), which induces the Toll pathway upon microbial infection, was markedly suppressed by miR-29-5p (Fig. 3-B). Similarly, miR-9-3p downregulated *GNBP1* expression (Fig. 3-D), while miR-971-3p and novel-m0019-3p significantly suppressed the expression of *PPO1* and *Toll3*, respectively (Fig. 3-E and F). Given the strong regulatory potentials of miR-71-5p and miR-7 on multiple immune genes, they were selected for subsequent investigations.

3.5. Spatiotemporal expression profiling of miR-71-5p and miR-7 and their putative targets

To study the relationships between miRNAs (miR-71-5p and miR-7) and their putative target genes (*ModSP1*, *Relish* and *Serine protease7*, *Lysozyme2*), we profiled their expression levels at different time intervals (6, 24, and 48 h), in various

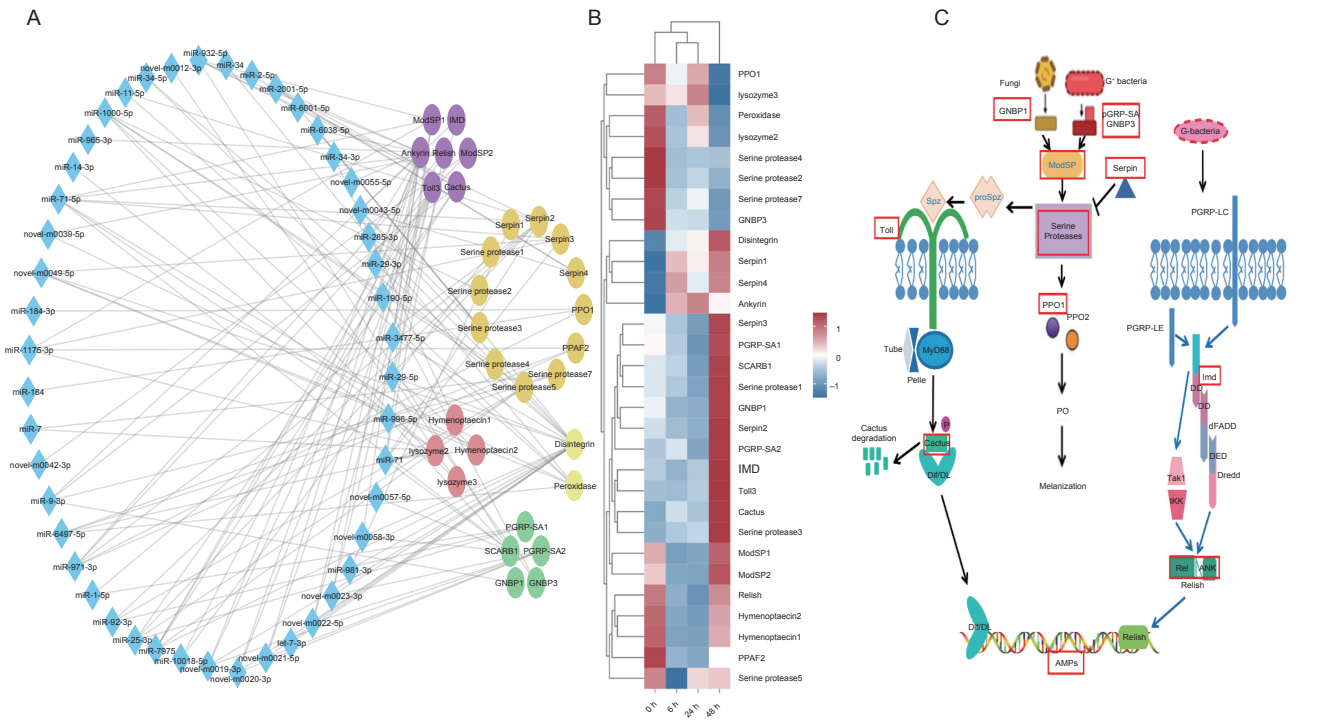


Fig. 2 Analysis of miRNA-mRNA regulatory networks, temporal expression of the target immune genes, and schematic representation of the associated pathways. A, miRNA-mRNA immune interaction generated using Cytoscape. Different colored circles (purple, yellow, red and green) represent target genes involved in antifungal immune responses, while blue diamonds indicate the miRNAs that regulate these genes. B, heatmap depicting the temporal expression of immune genes. Rows represent individual immune-related genes, while columns correspond to different post-infection time points. The color gradient from blue to red indicates expression levels, with blue representing low expression and red representing high expression. This analysis revealed dynamic changes in immune gene expression over time, particularly at 48 h. C, schematic representation of immune genes in different immune pathways, including the Toll and Imd signaling pathways. Red rectangles highlight the target genes of miRNAs identified in this study.

tissues (head, thorax, and abdomen) and life stages/castes (eggs, larvae, pupae, major, medium, minor, male and female) using qRT-PCR (Figs. 4 and 5).

The results showed that miR-71-5p levels rapidly increased relative to the expression of its target genes, *ModSP1* and *Relish*, which remained low at all intervals (Fig. 4-A), indicating a potential regulatory role of miR-71-5p in suppressing the expression of these immune-related genes. Similarly, tissue-specific profiling of miR-71-5p revealed its abundant expression in abdominal tissues compared to its target genes, *ModSP1* and *Relish* (Fig. 4-B). Furthermore, miR-71-5p exhibited significantly higher expressions in major worker ants with comparatively reduced *ModSP1* and *Relish* expression levels in all worker castes (Fig. 4-C). Notably, the significant reductions of miR-71-5p in both immature stages (eggs, larvae, and pupae) and adults (male and female), coupled with the relatively high abundances of *ModSP1* and *Relish* during developmental stages (Fig. 4-C), suggest a complex regulatory interplay between miR-71-5p and its target immune genes in *S. invicta*. This inverse pattern implies that miR-71-5p may act as a suppressor of *ModSP1* and *Relish* expression, with its downregulation allowing enhanced immune gene activity.

miR-7 showed a significant inhibitory effect on *Lysozyme2*, an antimicrobial peptide, and *Serine protease 7*, a crucial proteolytic enzyme involved in signal transduction (Gorman and Paskewitz 2001), across all time intervals after *M. anisopliae* infection (Fig. 5-A). Tissue expression profiling showed the contrasting expression patterns of miR-7 and its target genes in different tissues, mainly the thorax and abdominal tissues (Fig. 5-B). Interestingly, miR-7 was predominantly present in all worker castes, and exhibited very high expression levels relative to its target genes, *Lysozyme2* and *Serine protease7* (Fig. 5-C). Given the strong regulatory interactions between miR-71-5pwith *Relish*/*ModSP1* and miR-7 with *Lysozyme2*/*Serine protease7*, their potential in regulating miRNA-mediated antifungal immune responses in *S. invicta* was further investigated.

3.6. Overexpression of miR-71-5p and miR-7 increases the susceptibility of *S. invicta* to *M. anisopliae* infection

Oral administration of miR-71-5p mimic followed by fungal infection showed that the overexpression of miR-71-5p (miR-71-5p mimic+*M. anisopliae*) could significantly downregulate the expression of *ModSP1* and *Relish* compared to the control group (NC+*M. anisopliae*) (Fig. 6-A). The survival assay demonstrated that the overexpression of miR-71-5p enhanced fungal susceptibility, reducing the survival rates to 19.10% as opposed to 43.25% in the control group (NC+*M. anisopliae*) (Fig. 6-B). Notably, inhibiting miR-71-5p (miR-71-5p inhibitor+*M. anisopliae*) upregulated *ModSP1*

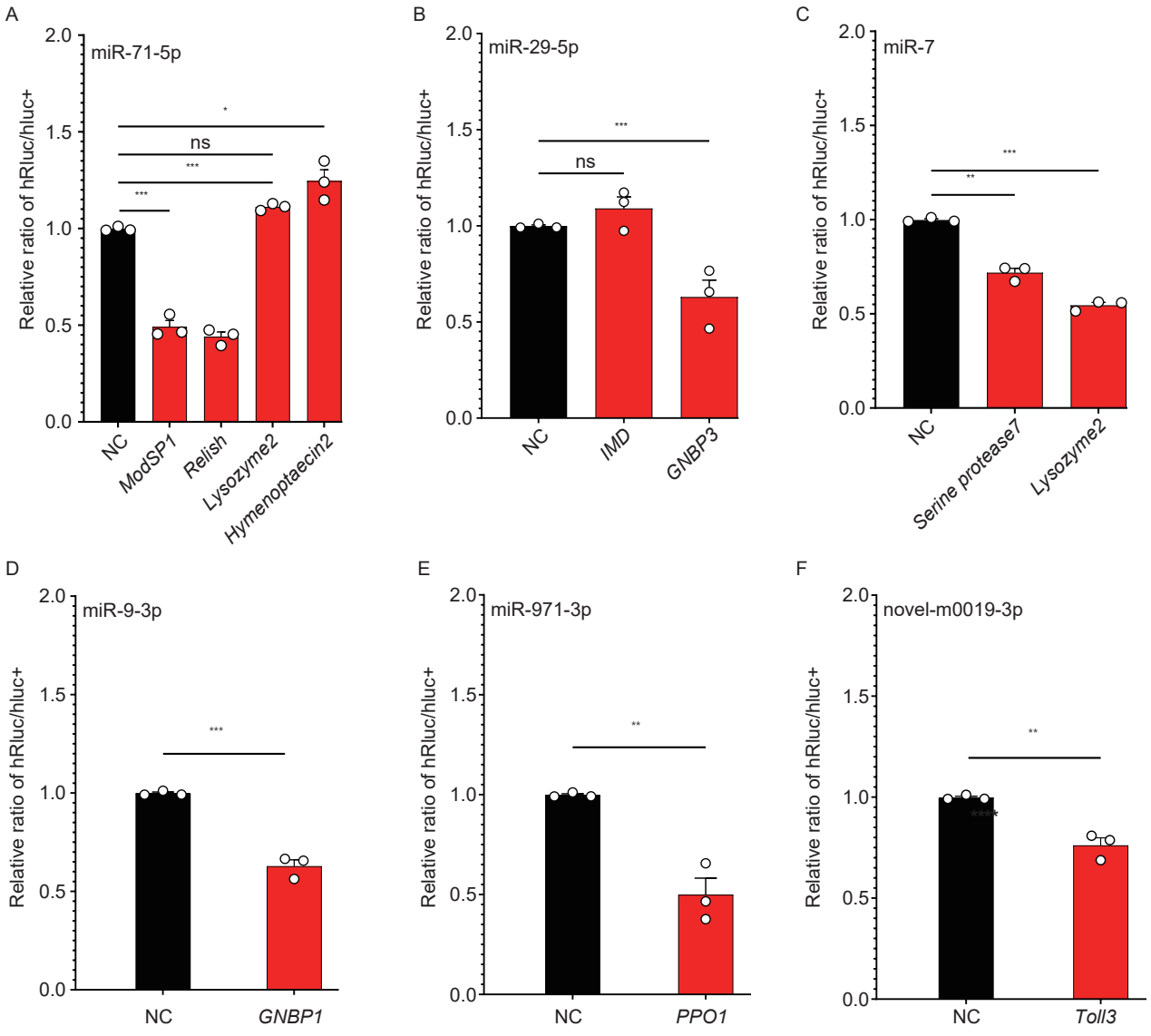


Fig. 3 *In vitro* dual-luciferase reporter assays of miRNA–mRNA interactions. A, interactions between miR-71-5p and *ModSP1, Relish*, *Lysozyme2* and *Hymenoptaecin2*. B, interaction between miR-29-5p and *IMD*/*GNBP3*. C, interaction between miR-7 and *Serine protease7*/*Lysozyme2*. D, interaction between miR-9-5p and *GNBP1*. E, interaction between miR-971-3p and *PPO1*. F, interaction between novel-m-0019-3p and *Toll3*. The relative luciferase expression ratios of firefly luciferase/Renilla luciferase (hRluc/hluc+) were calculated from three biological replicates (*n*=3). Statistical significance was determined by Student's *t*-test and compared with the negative control (NC). *, $P<0.05$; **, $P<0.01$; ***, $P<0.001$; ns, non-significant differences.

and *Relish* (Fig. 6-C) during fungal infection, implying that the absence of miR-71-5p influences the expression of these genes and likely offers partial protection against the adverse effects of *M. anisopliae* (Fig. 6-D).

Similarly, we profiled the expression of *Lysozyme2* and *Serine protease7* in the presence of miR-7 mimic at different time intervals. The results showed that overexpression of miR-7 efficiently suppressed *Lysozyme2*, particularly at 48 and 72 h after *M. anisopliae* infection, while *Serine protease7* exhibited significant reductions at all time intervals (Fig. 7-A). The survival assay showed that *S. invicta* exposed to *M. anisopliae* in the presence of elevated levels of miR-7 exhibited increased sensitivity to infection. The miR-7 overexpression group (miR-7 mimic+*M. anisopliae*) showed a significantly lower survival rate (16.16%) compared to the control group (NC+*M. anisopliae*) at 38.00%, signifying the potential role of miR-7 in enhancing fungal susceptibility (Fig. 7-B). To further establish the immunomodulatory function of miR-7, its expression in *S. invicta* was suppressed by employing the miR-7 inhibitor (Fig. 7-C). The results showed that the *S. invicta* immune response was significantly efficient in preventing *M. anisopliae* infection in the absence of miR-7 (miR-7 inhibitor+*M. anisopliae*), with 65.10% survival compared to 42.95% in the control group (NC+*M. anisopliae*), further strengthening our initial findings (Fig. 7-D).

Taken together, these findings demonstrated a crucial role of miR-71-5p and miR-7-mediated modulation of *Relish*/*ModSP1* and *Lysozyme2*/*Serine protease7*, respectively, which plays a critical role in determining *S. invicta* susceptibility to *M. anisopliae* infection.

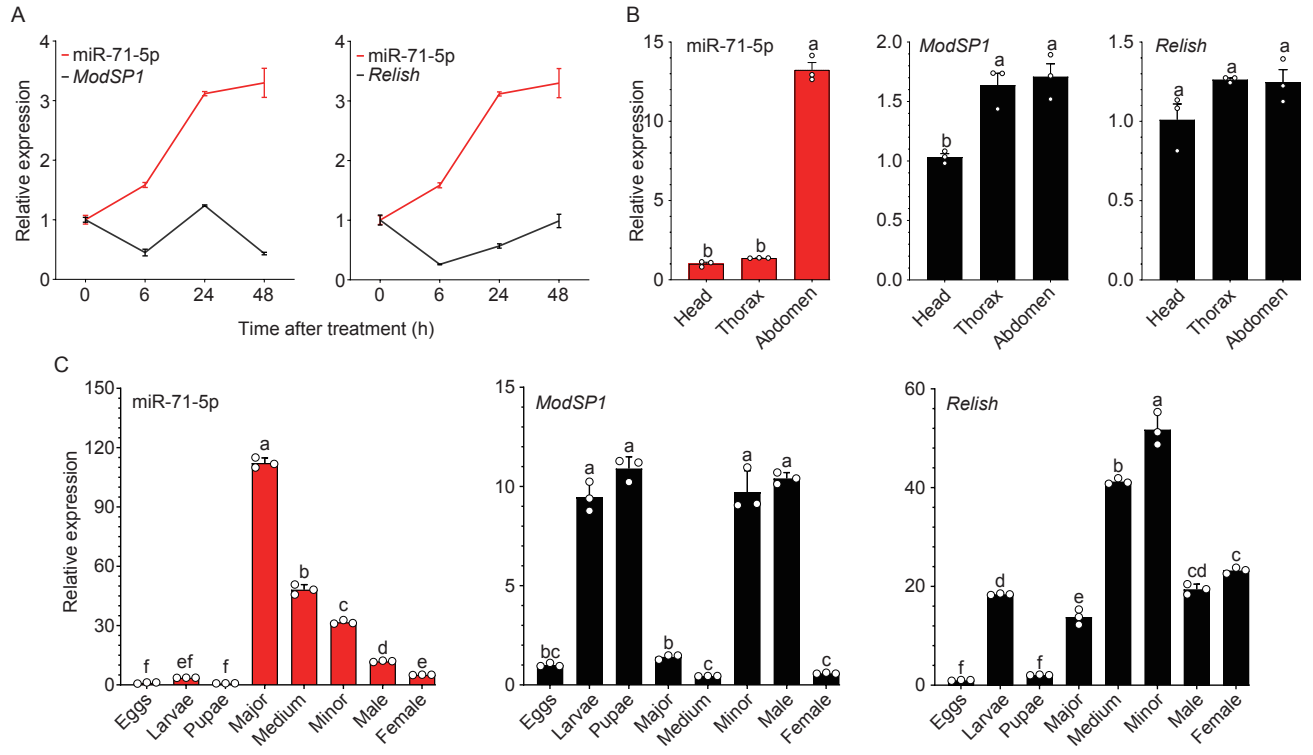


Fig. 4 Spatiotemporal profiling of miR-71-5p and its target immune genes. A, correlations between miR-71-5p and its target genes *ModSP1* and *Relish* at different time intervals after *Metarhizium anisopliae* infection. B, expression profiling of miR-71-5p and its target genes *ModSP1* and *Relish* in different tissues. C, expression profiling of miR-71-5p and its target genes *ModSP1* and *Relish* in different life stages and castes. Three biological samples were used as templates, and the data are presented as the mean±SEM. Different lowercase letters indicate significant differences (one-way ANOVA with Tukey's test; $P<0.05$).

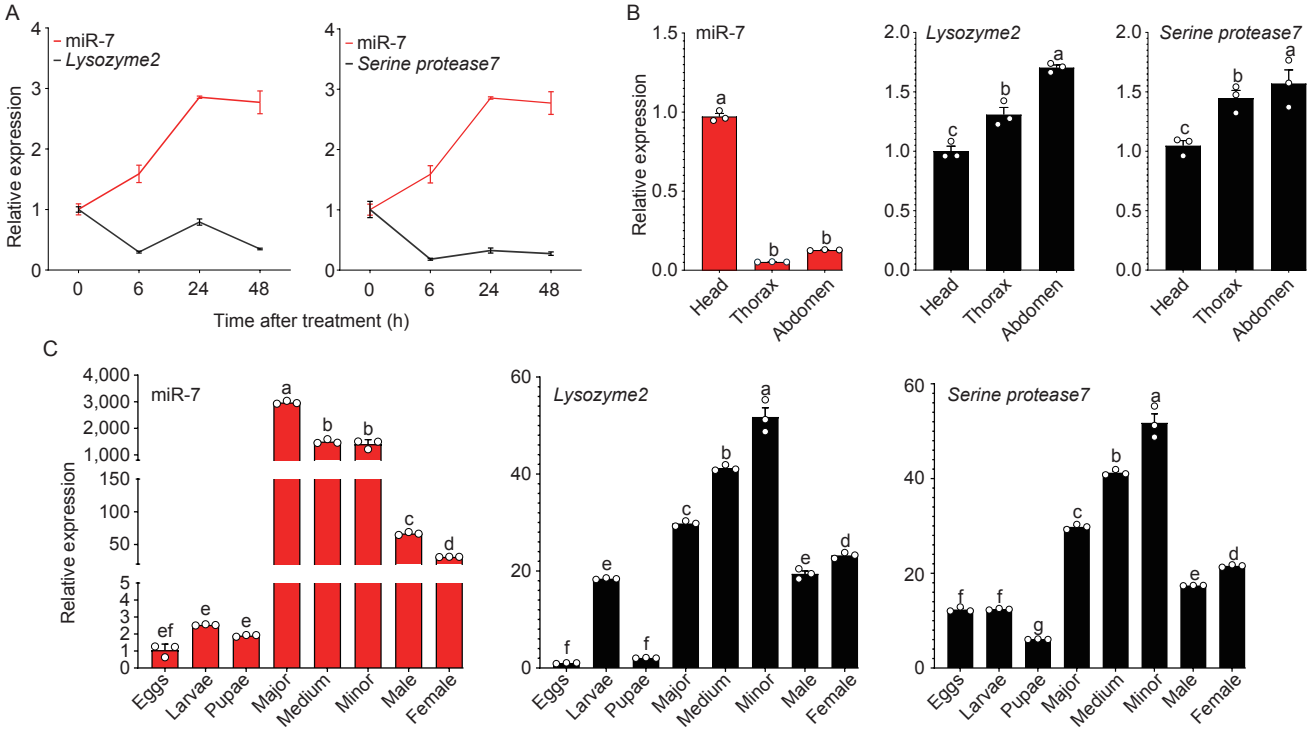


Fig. 5 Spatiotemporal profiling of miR-7 and its target immune genes. A, correlations between miR-7 and *Lysozyme2* and *Serine protease7* at different time intervals after *Metarhizium anisopliae* infection. B, expression profiling of miR-7 and its target immune genes (*Lysozyme2* and *Serine protease7*) in different tissues. C, expression profiling of miR-7 and its target genes *Lysozyme2* and *Serine protease7* in different life stages. Three biological samples were used as templates, and the data are presented as the mean±SEM. Different lowercase letters indicate significant differences (one-way ANOVA with Tukey's test; $P<0.05$).

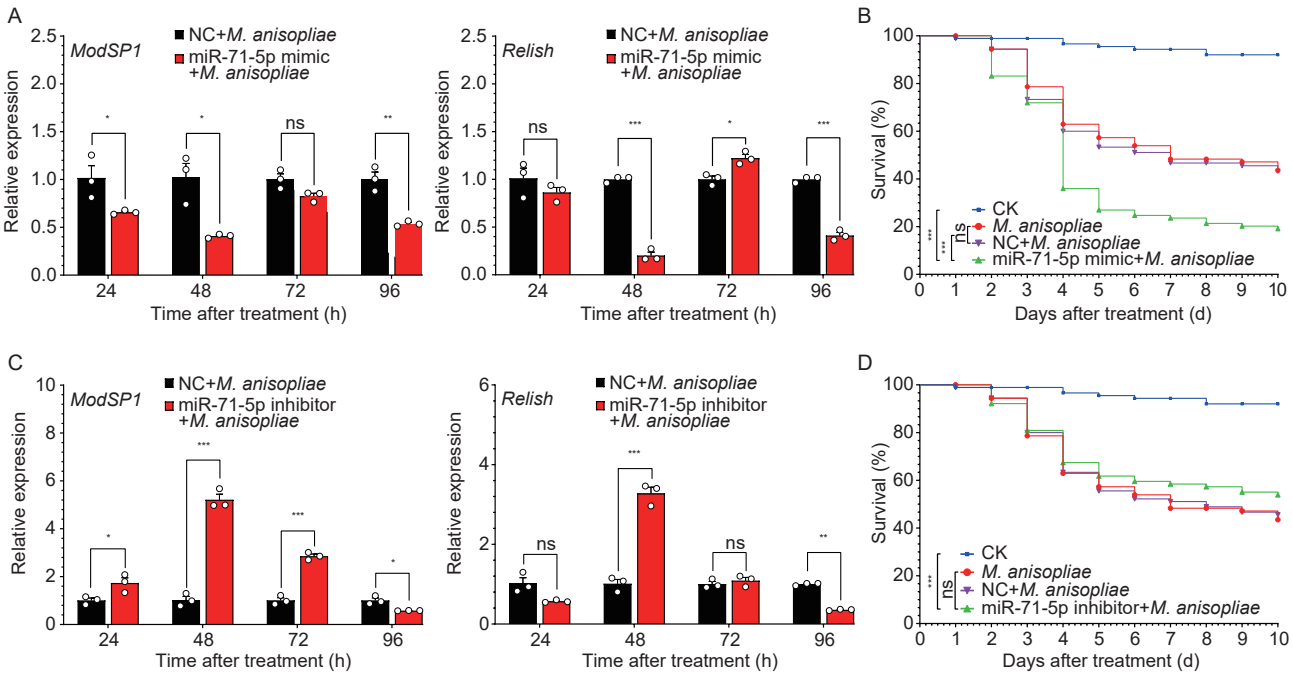


Fig. 6 Overexpression/inhibition of miR-71-5p and its effects on the target immune genes and survival of *Metarhizium anisopliae*-infected *Solenopsis invicta*. A, relative expression of *ModSP1* and *Relish* in miR-71-5p mimic administered *S. invicta* at different time intervals (24, 48, 72 and 96 h). B, survival percentages of miR-71-5p mimic administered *S. invicta* compared to control. C, relative expression of *ModSP1* and *Relish* in miR-71-5p inhibitor administered *S. invicta* at different time intervals (24, 48, 72 and 96 h). D, survival percentages of miR-71-5p inhibitor administered *S. invicta* compared to control. CK represents 0.05% Tween-80 control. NC represents negative control (scrambled mimic/inhibitor sequences). Survival curves were plotted using GraphPad Prism 10, and statistical significance was determined by the log-rank (Mantel-Cox) test. *, $P<0.05$; **, $P<0.01$; ***, $P<0.001$; ns, non-significant differences.

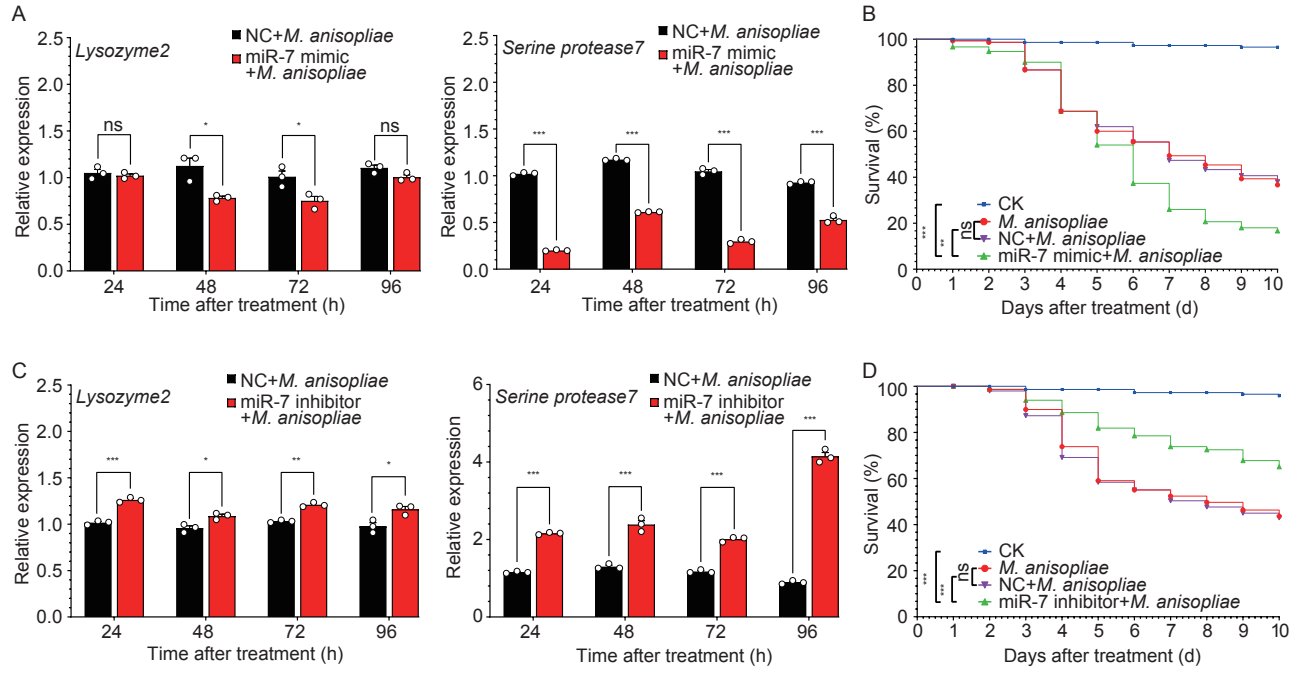


Fig. 7 Overexpression/inhibition of miR-7 and its effects on the target immune genes and survival of *Metarhizium anisopliae*-infected *Solenopsis invicta*. A, relative expression of *Lysozyme2* and *Serine protease7* in miR-7 mimic administered *S. invicta* at different time intervals. B, survival percentages of miR-7 mimic administered *S. invicta* compared to control. C, relative expression of *Lysozyme2* and *Serine protease7* in miR-7 inhibitor administered *S. invicta* at different time intervals. D, survival percentages of miR-7 inhibitor administered *S. invicta* compared to control. CK represents 0.05% Tween-80. NC represents negative control (scrambled mimic/inhibitor sequences). Survival curves were plotted using GraphPad Prism 10, and statistical significance was determined by the log-rank (Mantel-Cox) test. *, $P<0.05$; **, $P<0.01$; ***, $P<0.001$; ns, non-significant differences.

3.7. RNAi-mediated silencing of target immune genes

To elucidate the role of immune genes (*Relish*, *ModSP1*, *Lysozyme2* and *Serine protease7*) in *M. anisopliae*-infected *S. invicta*, we knocked down their expression using RNAi. qRT-PCR was performed to determine whether RNAi-mediated suppression of the immune genes was successful. The results showed that *ModSP1* and *Relish* were efficiently silenced at 24-72 h (Fig. 8-A). Survival assays were performed to determine whether gene silencing impacted the survival potential of *S. invicta*. Suppressing *ModSP1* (ds*ModSP1*+*M. anisopliae*) significantly reduced the survival percentage (25%) compared to the control (47%) (ds*GFP*+*M. anisopliae*). Notably, silencing *Relish* (ds*Relish*+*M. anisopliae*) did not drastically enhance or reduce the fungal susceptibility of *S. invicta* (Fig. 8-B). Similarly, *Lysozyme2* and *Serine protease7* were efficiently knocked down (Fig. 9-A). The survival assay showed that in the absence of *Lysozyme2* (ds*Lysozyme2*+*M. anisopliae*)

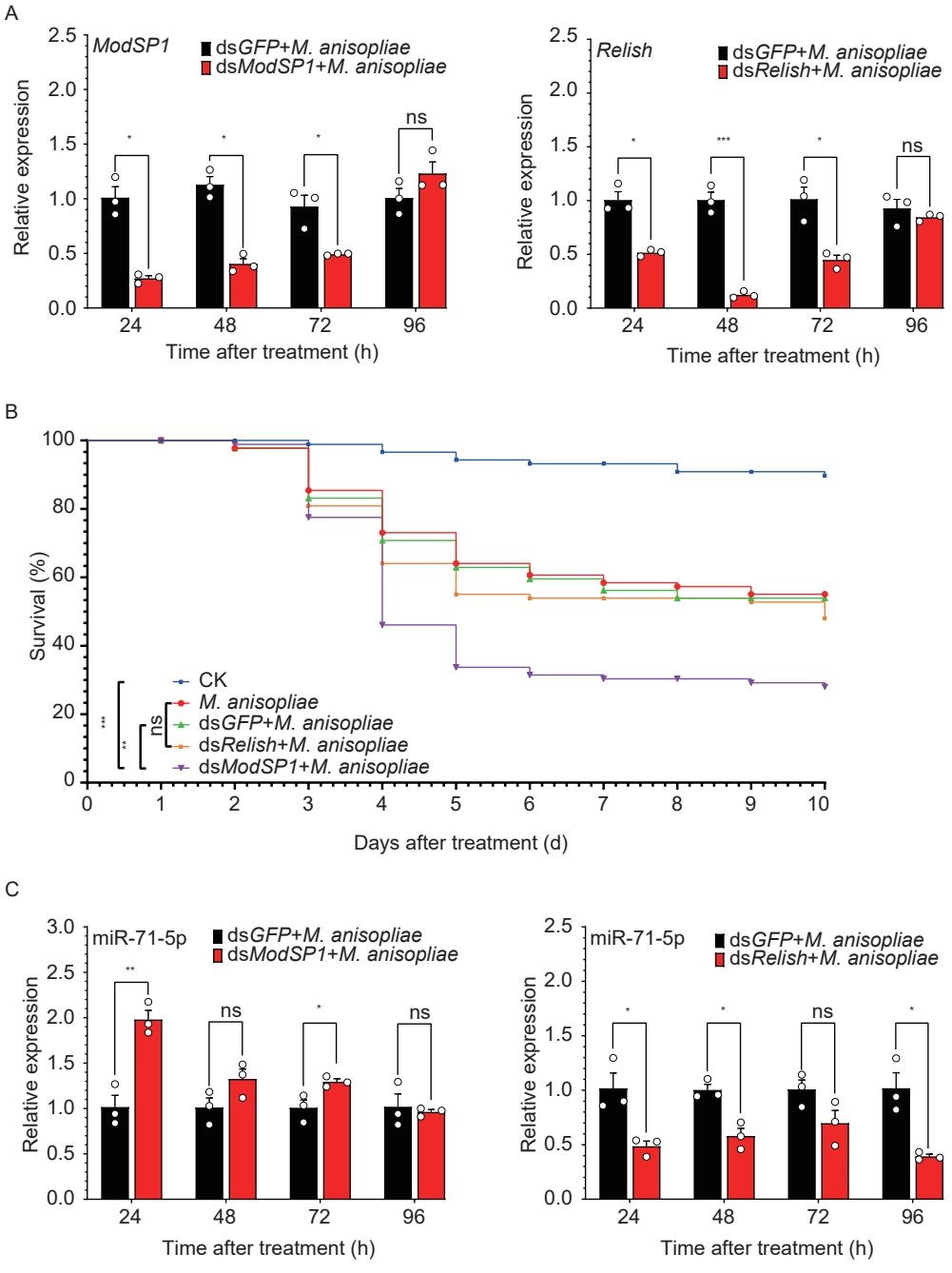


Fig. 8 RNAi-mediated silencing of *ModSP1* and *Relish* and its effect on the survival of *Solenopsis invicta*. A, relative expression of *ModSP1* and *Relish* in control and silenced groups during *Metarhizium anisopliae* infection. B, effects of RNAi-mediated silencing of *Relish* (ds*Relish*) and *ModSP1* (ds*ModSP1*) on survival of *M. anisopliae*-infected *S. invicta*. C, expression of miR-71-5p in *Relish* and *ModSP1* silenced groups at different time intervals. CK represents 0.05% Tween-80 control. Survival curves were plotted using GraphPad Prism 10, and statistical significance was determined by the log-rank (Mantel-Cox) test. *, $P<0.05$; **, $P<0.01$; ***, $P<0.001$; ns, non-significant differences.

and *Serine protease7* (ds*SP7+M. anisopliae*), *S. invicta* were significantly more susceptible to *M. anisopliae* infection, with accelerated mortality compared to the control group (ds*GFP+M. anisopliae*) (Fig. 9-B). These findings further solidified the role of these immune genes in the antifungal immune response in *S. invicta*.

Furthermore, we examined the expression levels of miR-71-5p and miR-7 in the *Relish*, *ModSP1*, *Lysozyme2* and *Serine protease7* silenced groups. The results revealed substantial alterations in miRNA levels compared to the control (Figs. 8-C and 9-C), suggesting a potential regulatory interplay. This interplay could involve feedback loops, regulatory crosstalk, compensatory mechanisms, miRNA dysregulation, or secondary effects on transcriptional regulation (Lai *et al.* 2016; Liu *et al.* 2023b). Determining which mechanisms are involved will require further in-depth experimental investigations, including temporal analysis, pathway-specific modulation studies, and integrative

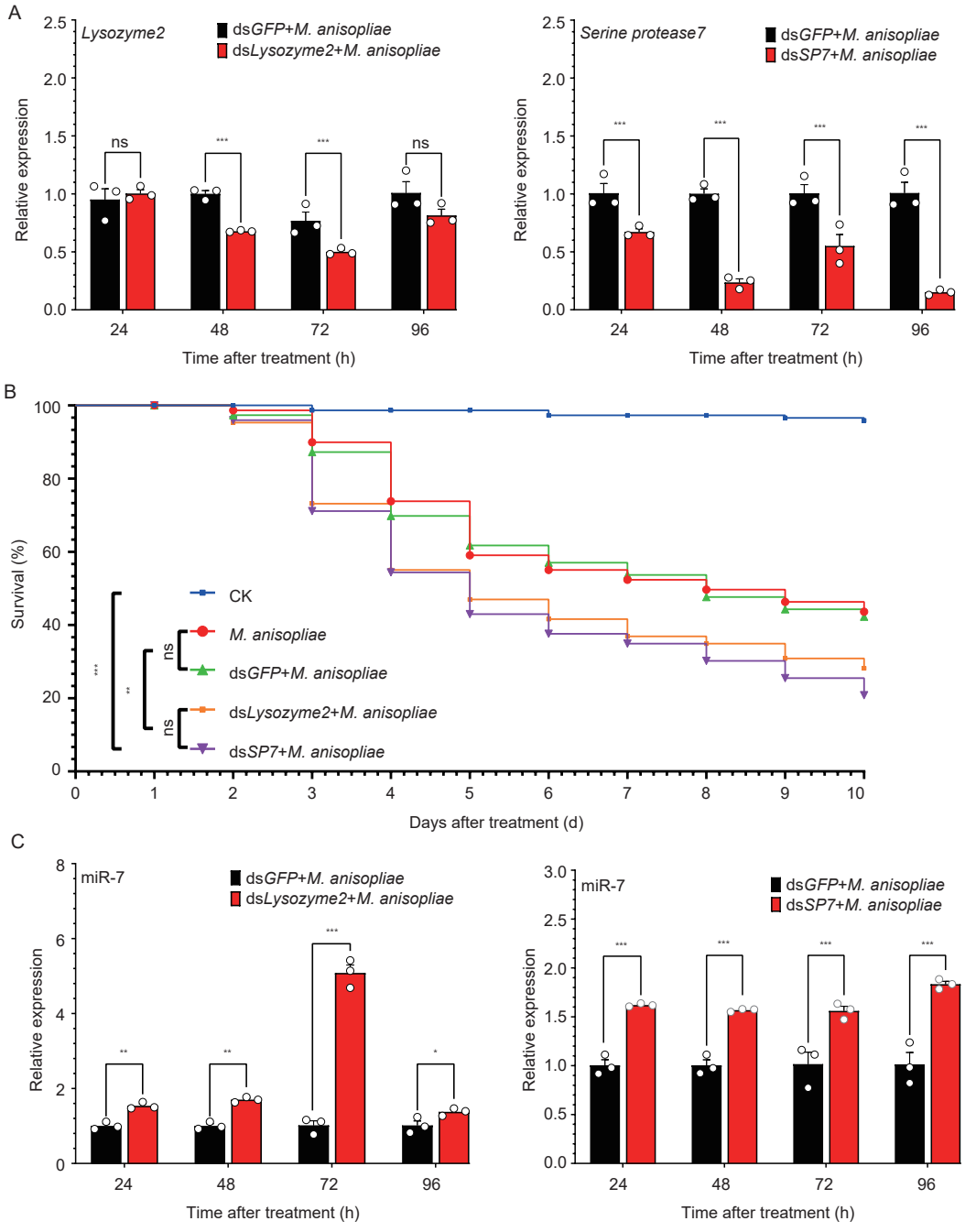


Fig. 9 RNAi-mediated silencing of *Lysozyme2* and *Serine protease7* and its effect on the survival of *Solenopsis invicta*. A, relative expression of *Lysozyme2* and *Serine protease7* in control and silenced groups during *Metarhizium anisopliae* infection. B, effects of RNAi-mediated silencing *Lysozyme2* (ds*Lysozyme2*) and *Serine protease7* (ds*SP7*) on survival of *M. anisopliae*-infected *S. invicta*. C, expression of miR-7 in *Lysozyme2* and *Serine protease7* silenced groups at different time intervals. CK represents 0.05% Tween-80. Survival curves were plotted using GraphPad Prism 10, and statistical significance was determined by the log-rank (Mantel-Cox) test. *, $P<0.05$; **, $P<0.01$; ***, $P<0.001$; ns, non-significant differences.

approaches combining transcriptomics and proteomics.

4. Discussion

MiRNAs are the most influential players in insect RNAi-mediated defense mechanisms, orchestrating a sophisticated co-evolutionary host-pathogen interplay (Jain *et al.* 2014). This study investigated the miRNA-mediated innate immune responses in *M. anisopliae*-infected *S. invicta*, focusing primarily on major worker ants which act as the colony's defense force. Temporal expression profiling of *M. anisopliae*-infected *S. invicta* revealed variations in the miRNAs at all time intervals (6, 24, and 48 h). Studies have shown that entomopathogens can induce changes in miRNA numbers and expression in both social insects, such as *Apis mellifera* (Guo *et al.* 2019), and solitary insects, such as *Plutella xylostella* (Zafar *et al.* 2021) and *Nilaparvata lugens* (Xie *et al.* 2021), demonstrating the widespread immunomodulatory potential of miRNAs during host–pathogen interactions. Some host-encoded miRNAs confer a survival advantage when combating entomopathogens. For instance, *Anopheles stephensi* translocate miR-100 and let-7 into *B. bassiana* hyphae to inhibit the two virulence-related genes (*sec2p* and *C6TF*) and enhance survival (Wang *et al.* 2021). On the contrary, some pathogen-induced host-miRNAs can weaken host immune responses to facilitate infection. For example, in *Aedes albopictus*, the dengue virus (DENV) exploits miR-281 to facilitate its replication, suggesting that the pathogen can manipulate host-encoded miRNAs for its advantage (Zhou *et al.* 2014).

Transcriptomic studies similar to ours have revealed an intricate role of the Toll pathway in the immune responses in social insects. Notably, young honeybees infected with the Israeli Acute Paralysis virus (IAPV) displayed elevated Toll expression compared to unaffected mature bees (Brutscher *et al.* 2015; Galbraith *et al.* 2015; Holmes and Johnston 2021). Recent research on the invasive Argentine ant, *Linepithema humile*, and *S. invicta* identified Toll, IMD, apoptosis and antimicrobial secretions as pivotal immune responses against microbial pathogens (Lester *et al.* 2019; Holmes and Johnston 2023). This pattern appears consistent for *S. invicta* in response to *M. anisopliae* infection, and we identified several differentially expressed miRNAs as potential regulators of the genes involved in multiple immune pathways. For instance, differentially expressed miR-6497-5p, which was predicted to regulate *Lysozyme2* and *Peroxidase2* in our studies, has previously been reported to target several immune genes in silkworms (*serpin-3*, *serpin-20*, *iap*, and *PGRP-S1*) (Zhao Z M *et al.* 2022). miR-1000 is crucial in regulating apoptosis and viral infection in *Marsupenaeus japonicas* (Gong *et al.* 2015), and it was also among the immune-related miRNAs and predicted to be a regulator of *Serine protease2*. Also, miR-11, which was identified in our data, has previously been reported to regulate several immune genes in *D. melanogaster* (Fullaondo and Lee 2012).

The regulatory relationships between miRNAs and genes are complex and multifaceted, with individual miRNAs capable of targeting multiple genes (Lai *et al.* 2016). We found that miR-71-5p is involved in regulating components of the IMD/Toll pathways, such as *Relish* and *ModSP1*. Survival assays demonstrated that overexpression of miR-71-5p significantly suppressed the expression of these target genes and increased fungal susceptibility in *S. invicta*. In the IMD signaling pathway, *Relish* (an NF-κB transcription factor) is transcribed into the nucleus and regulates the expression of antimicrobial peptides. Destruxin A, a cyclodepsipeptidic mycotoxin released by *M. anisopliae,* has shown to induce the expression of *Relish* in *B. mori* (Hu *et al.* 2016). Suppression of *Relish* likely reduces the expression of antimicrobial peptides and diminishes the defense against infectious microbes (Imler 2014). Similarly, knockdown of *Relish* in *Anthonomus grandis* (*AgraRelish*) (Moreira-Pinto *et al.* 2021) and *Aedes aegypti* (*Rel1* and *Rel2*) significantly accelerated *M. anisopliae*-induced mortality (Mehmood *et al.* 2023). *ModSP* is a modular serine protease that is a crucial component of insect innate immunity. Upon recognition of pathogen-associated molecular patterns (PAMPs), these proteases are sequentially activated in a cascade, initiating the immune pathways for prophenoloxidase (PPO) activation and antimicrobial peptide production *via* the Toll signaling pathway (Lemaitre and Hoffmann 2007). The transcription level of *ModSP* significantly increased in *B. bassiana*-infected *Ae. aegypti*, while its knockdown resulted in reduced antimicrobial peptide levels and survival (Lu *et al.* 2024).

MiR-71 has demonstrated its versatile regulatory potential in various invertebrates, including insects. In silkworms, miR-71 modulates the antiviral immune response by targeting the Seroin2 protein, thereby altering viral infectivity (Singh 2021). Enhancing miR-71 expression in *Culex pipiens* increased the sensitivity of mosquitoes to deltamethrin (Hong *et al.* 2014), signifying its possible involvement in the insect stress response. In western flower thrips, miR-71 disrupts chitin biosynthesis leading to high mortality when ingested (Kim *et al*. 2023). Similarly, miR-71 and miR-263 act as regulators of molting by suppressing the transcript levels of *CHS1* and *CHT10*, thus influencing chitin metabolism and potentially providing new targets for controlling locust plagues (Yang *et al.* 2016). In termites, miR-71 appears to be crucial for social immunity, as its stimulation weakens antifungal defenses and increases mortality during fungal infection (Liu *et al.* 2023b), further stressing its role in innate immunity.

MiR-7 is an evolutionarily conserved miRNA with a seed region of "-GGAAG-" that has been explored in vertebrates and invertebrates. In vertebrates, miR-7 suppresses malignant tumors by regulating various genes associated with signaling pathways (Zhao *et al.* 2015). In *Galeruca daurica*, a pest species of the Inner Mongolian grasslands, miR-7 targets *MARK2*, thereby participating in the regulation of larval-pupal metamorphosis (Wang *et al.* 2024). It has also shown potential in modulating the pathogen-induced immune response in *Apostichopus japonicus* (a marine invertebrate) by targeting *PAK1* (Zhao T *et al.* 2022). In this study, we functionally evaluated miR-7-*Lysozyme2*/*Serine protease7* regulatory axis due to their higher co-expression across all worker castes. The results showed that overexpression of miR-7 inhibited the expression of *Lysozyme2* and *Serine protease7*, thereby hindering

the immune response and accelerating *M. anisopliae*-induced mortality in *S. invicta*. Notably, the absence of miR-7 yielded no significant changes. However, changes in *Serine protease 7*, a gene encoding a melanization pathway component, reduced survival in *Drosophila* infected with *Listeria monocytogenes* (Ayres and Schneider 2008). *Serine protease* 7 was significantly upregulated in *Ostrinia furnacalis* upon *B. bassiana* infection (Zhang *et al.* 2022). Such pathogen-induced expression variations of serine proteases among different species could be attributed to differences in the microbial strains, infection dynamics, or ecological factors. Lysozymes have also been implicated in social immunity in burying beetles, *Nicrophorus vespilloides,* and bumblebees, *Bombus terrestris* (Richter *et al.* 2012; Palmer *et al.* 2016). Similarly, *Hymenoptaecin* has been documented in honeybee workers infected with *Nosema apis* (Moreira-Pinto *et al.* 2021), indicating the vital role of antimicrobial peptides in antifungal innate immunity. Furthermore, we observed a regulatory interplay where the miR-71-5p and miR-7 levels increased when their target genes were depleted. This finding is supported by similar observations in published studies. Specifically, the miR-285-Yki/Mask feedback loop demonstrates a comparable mechanism in *Drosophila*, i.e., the depletion of Yki or Mask leads to increased miR-285 expression. This suggests that miRNAs can be upregulated in response to the depletion of their target genes as part of a double-negative feedback loop (Li *et al.* 2017). However, confirming this would require further investigation.

MiRNA-mediated gene silencing has shown promising results for managing eusocial insect pest infestations. Genetically engineered *B. bassiana* expressing mosquito miRNAs (miR-8 and miR-375) suppressed the host Toll immune response and facilitated infection (Cui *et al.* 2022), so it represents a potential pathogen-mediated RNAi strategy for utilizing fungal-based biocontrol agents. RNAi-induced silencing of *termicin*, *GNBP2*, *TG*, *IDH*, and other coding genes in combination with *Metarhizium* could substantially enhance the vulnerability of nestmates to socially transmitted fungal conidia, consequently leading to elevated infection and mortality rates. Overexpression of *M. anisopliae*-induced miR-71a-5p, miR-7885-5p, and miR-252b downregulated defense genes and increased the mortality risk of termites (Liu *et al.* 2023a, b). Hence, miRNA-mediated immunity in social insects can affect their susceptibility to entomopathogenic fungi, which could be an effective tool for the biological control of fire ants.

5. Conclusion

We explored the molecular mechanisms involved in *M. anisopliae* and *S. invicta* interactions. Several fungus-induced miRNAs were found to be involved in modulating immune pathways. We demonstrated the feasibility of utilizing host miRNAs *via* dietary intake to reduce the immune response, thereby improving the biological control of *S. invicta* using *M. anisopliae*. Specifically, applying highly expressed miR-71-5p and miR-7 hampered the immune response and accelerated mortality in *S. invicta* major worker ants. Therefore, harnessing the host miRNA machinery could potentiate the effectiveness of current biocontrol agents by subverting host defense mechanisms and paving the way for developing advanced biotechnology-based biological control programs. This study was limited to major worker ants, so further research is needed to investigate caste-specific immune responses and practical field-level application methods.

Acknowledgements

This work was supported by grants from the National Natural Science Foundation of China (32172498 and W2433052), the National Key R&D Program of China (2021YFD1000500), and the Natural Science Foundation of Guangdong, China (2023A1515010305). We thank the editors and anonymous referees for their invaluable comments and suggestions.

Declaration of competing interest

The authors declare that they have no conflict of interest.

Declaration of generative AI and AI-assisted technologies in the writing process

The authors declare that they did not use AI in the preparation and writing of this manuscript.

Ethical statements

All applicable international, national and institutional guidelines for the care and use of animals were followed.

Appendices associated with this paper are available at https://doi.org/10.1016/j.jia.2025.02.009

References

Asgari S. 2011. Role of microRNAs in insect host–microorganism interactions. *Frontiers in Physiology*, **2**, 48.

Asgari S. 2018. Chapter two-microRNAs as regulators of insect host–pathogen interactions and immunity. In: Smagghe G, ed., *Advances in Insect Physiology*. Academic Press, London, England. pp. 19–45.

Ayres J S, Schneider D S. 2008. A signaling protease required for melanization in *Drosophila* affects resistance and tolerance of Infections. *PLoS Biology*, **6**, e305.

Bartel D P. 2004. MicroRNAs: Genomics, biogenesis, mechanism, and function. *Cell*, **116**, 281–297.

Betel D, Koppal A, Agius P, Sander C, Leslie C. 2010. Comprehensive modeling of microRNA targets predicts functional non-conserved and non-canonical sites. *Genome Biology*, **11**, R90.

Brutscher L M, Daughenbaugh K F, Flenniken M L. 2015. Antiviral defense mechanisms in honey bees. *Current Opinion in Insect Science*, **10**, 71–82.

Chen J, Zhou Y, Lei Y, Shi Q, Qi G, He Y, Lyu L. 2022. Role of the foraging gene in worker behavioral transition in the red imported fire ant, *Solenopsis invicta* (Hymenoptera: Formicidae). *Pest Management Science*, **78**, 2964–2975.

Cremer S, Armitage S A, Schmid-Hempel P. 2007. Social immunity. *Current Biology*, **17**, R693–R702.

Cui C, Wang Y, Li Y, Sun P, Jiang J, Zhou H, Liu J, Wang S. 2022. Expression of mosquito miRNAs in entomopathogenic fungus induces pathogen-mediated host RNA interference and increases fungal efficacy. *Cell Reports*, **41**, 111527.

Etebari K, Asgari S. 2013. Conserved microRNA miR-8 blocks activation of the Toll pathway by upregulating Serpin 27 transcripts. *RNA Biology*, **10**, 1356–1364.

Evans J D, Aronstein K, Chen Y P, Hetru C, Imler J L, Jiang H, Kanost M, Thompson G J, Zou Z, Hultmark D. 2006. Immune pathways

and defence mechanisms in honey bees *Apis mellifera*. *Insect Molecular Biology*, **15**, 645–656.
Fang W, Azimzadeh P, Leger R J S. 2012. Strain improvement of fungal insecticides for controlling insect pests and vector-borne diseases. *Current Opinion in Microbiology*, **15**, 232–238.
Feldhaar H, Gross R. 2008. Immune reactions of insects on bacterial pathogens and mutualists. *Microbes and Infection*, **10**, 1082–1088.
Freitak D, Knorr E, Vogel H, Vilcinskas A. 2012. Gender- and stressor-specific microRNA expression in *Tribolium castaneum*. *Biology Letters*, **8**, 860–863.
Friedländer M R, Mackowiak S D, Li N, Chen W, Rajewsky N. 2011. miRDeep2 accurately identifies known and hundreds of novel microRNA genes in seven animal clades. *Nucleic Acids Research*, **40**, 37–52.
Fullaondo A, Lee S Y. 2012. Identification of putative miRNA involved in *Drosophila melanogaster* immune response. *Developmental & Comparative Immunology*, **36**, 267–273.
Galbraith D A, Yang X, Niño E L, Yi S, Grozinger C. 2015. Parallel epigenomic and transcriptomic responses to viral infection in honey bees (*Apis mellifera*). *PLoS Pathogens*, **11**, e1004713.
Geng T, Lu F, Wu H, Lou D, Tu N, Zhu F, Wang S. 2021. Target antifungal peptides of immune signalling pathways in silkworm, *Bombyx mori*, against *Beauveria bassiana*. *Insect Molecular Biology*, **30**, 102–112.
Gong Y, Ju C, Zhang X. 2015. The miR-1000-p53 pathway regulates apoptosis and virus infection in shrimp. *Fish & Shellfish Immunology*, **46**, 516–522.
Gorman M J, Paskewitz S M. 2001. Serine proteases as mediators of mosquito immune responses. *Insect Biochemistry and Molecular Biology*, **31**, 257–262.
Guo R, Du Y, Zhou N H, Liu S Y, Xiong C L, Zheng Y Z, Fu Z M, Xu G J, Wang H P, Geng S H, Zhou D D, Chen D F. 2019. Comprehensive analysis of differentially expressed microRNAs and their target genes in the larval gut of *Apis mellifera* ligustica during the late stage of *Ascosphaera apis* stress. *Acta Entomologica Sinica*, **62**, 49–60. (in Chinese)
Hillyer J F. 2016. Insect immunology and hematopoiesis. *Developmental & Comparative Immunology*, **58**, 102–118.
Holmes V R, Johnston J S. 2021. The innate immune response of eusocial hymenopterans to viral pathogen challenge. *Annals of the Entomological Society of America*, **115**, 141–147.
Holmes V R, Johnston J S. 2023. Differential gene expression of innate immune response genes consequent to *Solenopsis invicta* virus-3 infection. *Genes*, **14**, 188.
Hong S, Guo Q, Wang W, Hu S, Fang F, Lv Y, Yu J, Zou F, Lei Z, Ma K, Ma L, Zhou D, Sun Y, Zhang D, Shen B, Zhu C. 2014. Identification of differentially expressed microRNAs in *Culex pipiens* and their potential roles in pyrethroid resistance. *Insect Biochemistry and Molecular Biology*, **55**, 39–50.
Hu W, He G, Wang J, Hu Q. 2016. The effects of destruxin A on relish and rel gene regulation to the suspected immune-related genes of silkworm. *Molecules*, **22**, 41.
Imler J L. 2014. Overview of *Drosophila* immunity: A historical perspective. *Developmental & Comparative Immunology*, **42**, 3–15.
Liang M R, Shuang Y M, Deng J F, Peng L Y, Zhang S Q, Zhang C, Xu, Y J, Lu Y Y, Wang L. 2023. Toxicity and horizontal transfer of bifenthrin and dimefluthrin against the red imported fire ant, *Solenopsis invicta* Buren (Hymenoptera: Formicidae), and the efficacy of their dust applications in the field. *Journal of Integrative Agricultur*e, **22**, 1465–1476.
Jain S, Rana V, Shrinet J, Sharma A, Tridibes A, Sunil S, Bhatnagar R K. 2014. Blood feeding and *Plasmodium* infection alters the miRNome of *Anopheles stephensi*. *PLoS ONE*, **9**, e98402.
Kim S J, Lee J H, Kim J H, Yoon K A, Lee S H. 2023. Ingestion of antagomir or agomir of microRNA results in physiological changes and high mortality in *Frankliniella occidentalis*. *Entomologia Generalis*, **43**, 109–116.
Lai X, Wolkenhauer O, Vera J. 2016. Understanding microRNA-mediated gene regulatory networks through mathematical modelling. *Nucleic Acids Research*, **44**, 6019–6035.
Lemaitre B, Hoffmann J. 2007. The host defense of *Drosophila melanogaster*. *Annual Review of Immunology*, **25**, 697–743.
Lester P J, Buick K H, Baty J W, Felden A, Haywood J. 2019. Different bacterial and viral pathogens trigger distinct immune responses in a globally invasive ant. *Scientific Reports*, **9**, 5780.
Lewis B P, Burge C B, Bartel D P. 2005. Conserved seed pairing, often flanked by adenosines, indicates that thousands of human genes are microRNA targets. *Cell*, **120**, 15–20.
Li D, Liu Y, Pei C, Zhang P, Pan L, Xiao J, Meng S, Yuan Z, Bi X. 2017. miR-285–Yki/Mask double-negative feedback loop mediates blood–brain barrier integrity in *Drosophila*. *Proceedings of the National Academy of Sciences of the United States of America*, **114**, E2365–E2374.
Liu L, Wang D H, Zhao C C, Yan F M, Lei C L, Su L J, Zhang Y C, Huang Q Y, Tang Q B. 2023a. Transcriptomics reveals the killing mechanism by which entomopathogenic fungi manipulate the RNA expression profiles of termites and provides inspiration for green pest management. *Journal of Agricultural and Food Chemistry*, **71**, 7152–7162.
Liu L, Yan F M, Zhao C C, Su L J, Huang Q Y, Tang Q B. 2023b. microRNAs shape social immunity: A potential target for biological control of the termite *Reticulitermes chinensis*. *Journal of Pest Science*, **96**, 265–279.
Lu H L, Leger R J S. 2016. Chapter seven-Insect immunity to entomopathogenic fungi. In: Lovett B, Leger R J S eds., *Advances in Genetics*. Academic Press, San Diego, CA, USA. pp. 251–285.
Lu T, Ji Y, Chang M, Zhang X, Wang Y, Zou Z. 2024. The accumulation of modular serine protease mediated by a novel circRNA sponging miRNA increases *Aedes aegypti* immunity to fungus. *BMC Biology*, **22**, 7.
Lucas K J, Zhao B, Liu S, Raikhel A S. 2015. Regulation of physiological processes by microRNAs in insects. *Current Opinion in Insect Science*, **11**, 1–7.
Mehmood N, Hassan A, Zhong X, Zhu Y, Ouyang G, Huang Q. 2023. Entomopathogenic fungal infection following immune gene silencing decreased behavioral and physiological fitness in *Aedes aegypti* mosquitoes. *Pesticide Biochemistry and Physiology*, **195**, 105535.
Menchetti M, Schifani E, Alicata A, Cardador L, Sbrega E, Toro-Delgado E, Vila R. 2023. The invasive ant *Solenopsis invicta* is established in Europe. *Current Biology*, **33**, R896–R897.
Moreira-Pinto C E, Coelho R R, Leite A G B, Silveira D A, de Souza D A, Lopes R B, Macedo L L P, Silva M C M, Ribeiro T P, Morgante C V, Antonino J D, Grossi-de-Sa M F. 2021. Increasing *Anthonomus grandis* susceptibility to *Metarhizium anisopliae* through RNAi-induced *AgraRelish* knockdown: A perspective to combine biocontrol and biotechnology. *Pest Management Science*, **77**, 4054–4063.
Mukherjee K, Vilcinskas A. 2014. Development and immunity-related microRNAs of the lepidopteran model host *Galleria mellonella*. *BMC Genomics*, **15**, 705.
Palmer W J, Duarte A, Schrader M, Day J P, Kilner R, Jiggins F M. 2016. A gene associated with social immunity in the burying beetle *Nicrophorus vespilloides*. *Proceedings of the Royal Society* (B: Biological Sciences), **283**, 20152733.
Qiu H L, Lu L H, Shi Q X, He Y R. 2014. Fungus exposed *Solenopsis invicta* ants benefit from grooming. *Journal of Insect Behavior*, **27**, 678–691.
Qiu H L, Lu L H, Shi Q X, Tu C C, Lin T, He Y R. 2015. Differential necrophoric behaviour of the ant *Solenopsis invicta* towards fungal-infected corpses of workers and pupae. *Bulletin of Entomological Research*, **105**, 607–614.
Qiu H L, Lu L H, Zalucki M, He Y R. 2016. *Metarhizium anisopliae* infection alters feeding and trophallactic behavior in the ant *Solenopsis invicta*. *Journal of Invertebrate Pathology*, **138**, 24–29.
Richter J, Helbing S, Erler S, Lattorff H M G. 2012. Social context-dependent immune gene expression in bumblebees (*Bombus terrestris*). *Behavioral Ecology and Sociobiology*, **66**, 791–796.
Robinson M D, McCarthy D J, Smyth G K. 2009. edgeR: A bioconductor package for differential expression analysis of digital gene expression data. *Bioinformatics*, **26**, 139–140.
Sakamoto H, Goka K. 2021. Acute toxicity of typical ant control agents to the red imported fire ant, *Solenopsis invicta* (Hymenoptera: Formicidae). *Applied Entomology and Zoology*, **56**, 217–224.
Schmid-Hempel P. 2005. Evolutionary ecology of insect immune defenses. *Annual Review of Entomology*, **50**, 529–551.
Scholte E J, Ng'Habi K, Kihonda J, Takken W, Paaijmans K, Abdulla S, Killeen G F, Knols B G. 2005. An entomopathogenic fungus for control of adult African malaria mosquitoes. *Science*, **308**, 1641–1642.
Singh C P. 2021. *In vitro* treatment of seroin proteins to BmNPV

budded virions suppresses viral proliferation in *Bombyx mori* larvae and ectopic overexpression of host-miRNAs downregulates the expression of Seroin2 mRNA in BmN cells. *International Journal of Tropical Insect Science*, **41**, 1485–1491.

Tschinkel W R. 2013. *The Fire Ants*. Harvard University Press, Cambridge, MA, USA.

Wang C, Wang S. 2017. Insect pathogenic fungi: Genomics, molecular interactions, and genetic improvements. *Annual Review of Entomology*, **62**, 73–90.

Wang H C, Li L, Zhang J H, Yao Z H, Pang B P. 2024. MicroRNA *miR-7-5p* targets MARK2 to control metamorphosis in *Galeruca daurica*. *Comparative Biochemistry and Physiology* (Part B: Biochemistry and Molecular Biology), **272**, 110967.

Wang Y, Cui C, Wang G, Li Y, Wang S. 2021. Insects defend against fungal infection by employing microRNAs to silence virulence-related genes. *Proceedings of the National Academy of Sciences of the United States of America*, **118**, e2023802118.

Wei G, Sun L, Li R, Li L, Xu J, Ma F. 2018. Dynamic miRNA-mRNA regulations are essential for maintaining *Drosophila* immune homeostasis during *Micrococcus luteus* infection. *Developmental & Comparative Immunology*, **81**, 210–224.

Wu H, Xu Y, Zafar J, Mandal S D, Lin L, Lu Y, Jin F, Pang R, Xu X. 2023. Transcriptomic analysis reveals the impact of the biopesticide *Metarhizium anisopliae* on the immune system of major workers in *Solenopsis invicta*. *Insects*, **14**, 701.

Xie J, Peng Y, Xia Y. 2021. Genome-wide identification and analysis of *Nilaparvata lugens* microRNAs during challenge with the entomopathogenic fungus *Metarhizium anisopliae*. *Journal of Fungi*, **7**, 295.

Yan Y, Aumann R A, Haecker I, Schetelig M F. 2023. CRISPR-based genetic control strategies for insect pests. *Journal of Integrative Agriculture*, **22**, 651–668.

Yang L, Yang L, Wang X, Peng C, Chen X, Wei W, Xu X, Ye G, Xu J. 2023. Toll and IMD immune pathways are important antifungal defense components in a pupal parasitoid, *Pteromalus puparum*. *International Journal of Molecular Sciences*, **24**, 14088.

Yang M, Wang Y, Jiang F, Song T, Wang H, Liu Q, Zhang J, Zhang J, Kang L. 2016. miR-71 and miR-263 jointly regulate target genes *Chitin synthase* and *Chitinase* to control locust molting. *PLoS Genetics*, **12**, e1006257.

Zafar J, Wu H, Xu Y, Lin L, Kang Z, Zhang J, Zhang R, Lu Y, Jin F, Xu X. 2023. Transcriptomic analysis of *Metarhizium anisopliae*-induced immune-related long non-coding RNAs in polymorphic worker castes of *Solenopsis invicta*. *International Journal of Molecular Sciences*, **24**, 13983.

Zafar J, Zhang Y, Huang J, Freed S, Shoukat R F, Xu X, Jin F. 2021. Spatio-temporal profiling of *Metarhizium anisopliae* —Responsive microRNAs involved in modulation of *Plutella xylostella* immunity and development. *Journal of Fungi*, **7**, 942.

Zhang S, Feng T, Ji J, Wang L, An C. 2022. Serine protease SP7 cleaves prophenoloxidase and is regulated by two serpins in *Ostrinia furnacalis* melanization. *Insect Biochemistry and Molecular Biology*, **141**, 103699.

Zhang Y, Tian T, Zhang K, Zhang Y J, Wu Q J, Xie W, Guo Z J, Wang S L. 2023. Lack of fitness cost and inheritance of resistance to abamectin based on the establishment of a near-isogenic strain of *Tetranychus urticae*. *Journal of Integrative Agriculture*, **22**, 1809–1819.

Zhang W, Ortiz-Urquiza A, Keyhani N O. 2021. Altered expression of chemosensory and odorant binding proteins in response to fungal infection in the red imported fire ant, *Solenopsis invicta*. *Frontiers in Physiology*, **12**, . 596571

Zhao J, Tao Y, Zhou Y, Qin N, Chen C, Tian D, Xu L. 2015. MicroRNA-7: A promising new target in cancer therapy. *Cancer Cell International*, **15**, 103.

Zhao T, Ren L, Li C, Liu L, Zou Y, Yan H, Zhan Y, Chang Y. 2022. MiR-7 regulates pathogen-induced immune response via PAK1 in the sea cucumber *Apostichopus japonicus*. *Frontiers in Immunology*, **13**, 927796.

Zhao Z M, Yin H T, Shen M M, Zhang S L, Chen Z K, Li T, Zhang Z D, Zhao W G, Guo X J, Wu P. 2022. Transcriptome of miRNA during inhibition of *Bombyx mori* nuclear polyhedrosis virus by geldanamycin in BmN cells. *Archives of Insect Biochemistry and Physiology*, **110**, e21880.

Zheng X, Li S, Si Y, Hu J, Xia Y. 2020. Locust can detect *β*-1, 3-glucan of the fungal pathogen before penetration and defend infection via the Toll signaling pathway. *Developmental & Comparative Immunology*, **106**, 103636.

Zhou Y, Liu Y, Yan H, Li Y, Zhang H, Xu J, Puthiyakunnon S, Chen X. 2014. miR-281, an abundant midgut-specific miRNA of the vector mosquito *Aedes albopictus* enhances dengue virus replication. *Parasites & Vectors*, **7**, 488.

Executive Editor-in-Chief Fanghao Wan
Managing Editor Lujuan Sun